Published in final edited form as:
Cell. 1989 April 7; 57(1): 177–187.

Genetic Control of Cell Division Patterns in the Drosophila Embryo

Bruce A. Edgar and **Patrick H. O'Farrell**
Department of Biochemistry and Biophysics, University of California, San Francisco, California 94143

Summary

In Drosophila embryogenesis, mitotic control undergoes a significant transition during the 14th interphase. Mitoses before interphase 14 run on maternal products, and occur in metasynchronous waves. Mitoses after interphase 14 require zygotic transcription, and occur asyncronously in an intricate, highly ordered spatio–temporal pattern. Mutations at the *string* (*stg*) locus cause cell-cycle arrest during this transition, in G2 of interphase 14, yet do not arrest other aspects of development. This phenotype suggests that *stg* is required specifically for initiating mitosis. We describe the cloning of *stg*, and show that its predicted amino acid sequence is homologous to that of *cdc25*, a regulator of mitotic initiation in the yeast S. pombe. In addition, we show that zygotic expression of *stg* mRNA occurs in a dynamic series of spatial patterns which anticipate the patterns of the zygotically driven cell divisions. Therefore we suggest that regulated expression of *stg* mRNA controls the timing and location of these embryonic cell divisions.

Introduction

The development of a multicellular organism from a single egg cell involves an extended series of precisely regulated cell divisions. Cell lineages leading to different organs and tissue types divide according to distinct spatial and temporal patterns, which we assume are somehow specified in the "genetic program" of development. Although the patterns of embryonic cell divisions have been studied in detail in several organisms (Sulston et al., 1983; Hartenstein and Campos-Ortega, 1985; Weisblat et al., 1980), very little is known about their regulation by molecular and genetic mechanisms. We are studying this problem in Drosophila embryos because they have a well-characterized pattern of cell proliferation which may be investigated using an excellent array of cytological, genetic, and molecular techniques. Moreover, certain features of the embryonic cell division program in Drosophila seem to be evolutionary conserved. A period of rapid synchronous cleavages followed by a transition to slower, asynchronous cell divisions, for instance, occurs during early development in organisms as distantly related as marine invertebrates, insects, amphibians, and birds (Mita, 1983; Edgar et al., 1986a; Newport and Kirschner, 1982; Olszanska et al., 1984). Such phenomenological similarities may well reflect common molecular mechanisms, since many of the genes involved in mitotic control are highly conserved in eukaryotes as diverse as yeast, flies, and humans (Lee and Nurse, 1988; Lehner and O'Farrell, 1989; Dunphy and Newport, 1988c).

Drosophila development begins with 13 extremely rapid mitotic waves that traverse the embryo, dividing the nuclei in a single cytoplasm without cytokinesis (Rabinowitz, 1941). The first extended interphase (interphase 14) occurs about 2 hr after fertilization, and it is during this period that high levels of transcription first occur and cells form around the embryonic nuclei. Following interphase 14, these cells enter mitosis over a period of about 2 hr, in a precisely regulated spatio–temporal pattern that reflects newly established differences in cell identities (Foe and Alberts, 1983; Foe, 1989). Most cell lineages have three embryonic divisions after interphase 14, but some, such as the neurogenic lineages, undergo as many as

six divisions, and others, such as the amnioserosa, never divide again (Hartenstein and Campos-Ortega, 1985).

While previous studies revealed little about how the patterns of these divisions are controlled, they suggested that cell-cycle progression in the early embryo is regulated by factors that trigger mitosis. Experiments with translation inhibitors, for instance, showed that during the rapid cleavages in Drosophila and Xenopus embryos new proteins are required for the initiation of each mitosis, but not for the initiation or completion of S phases (Newport and Kirschner, 1984; Edgar and Schubiger, 1986). In accordance with this result, Harland and Laskey (1980) and Blow and Laskey (1988) found that the cytoplasm of cleavage-stage Xenopus embryos is constitutive in its ability to support DNA replication, and proposed that S phases during the cleavages are triggered simply by nuclear envelope breakdown during mitosis.

This simple mode of regulation, with a single control point at the G2/M transition, seems to continue during the later asynchronous cell cycles. Cycle 14, the first spatially patterned cell cycle in Drosophila, begins after a synchronous mitosis, lacks G1, and has a short S phase that begins and ends virtually synchronously in all the embryonic nuclei (Blumenthal et al., 1974; McKnight and Miller, 1977; Edgar and Schubiger, 1986; Edgar, unpublished data). Consequently, patterned variation in cell-cycle lengths during cycle 14 results from differences in the lengths of G2 periods, which vary between 30 and >150 min in different cells. This may continue to be true at least through cycle 15, which also lacks a detectable G1 phase (Edgar, unpublished data). As in the early synchronous divisions, blocking protein synthesis during cycle 14 results in G2 arrest, again suggesting that new factors are required only to initiate mitosis (Edgar, unpublished data). This type of cell-cycle regulation is significantly different from that found in budding yeast and many types of cultured cells, where control occurs primarily at the G1/S boundary (see Murray, 1987, for review).

Another clue to the developmental regulation of the cell-cycle comes from experiments with the transcription inhibitor α-amanitin. These experiments indicate that maternal mRNAs are sufficient to drive the first 13 nuclear divisions, and that zygotic mRNAs are first required to initiate the patterned cell divisions of mitosis 14 (Gutzeit, 1980; Edgar et al., 1986a; Edgar, unpublished data). This conclusion is supported by genetic studies which show that mitoses 1–13 can be perturbed by maternal-effect mutations (Zalokar et al., 1975), but not by deficiencies in the zygotic genome (Wieschaus and Sweeton, 1988; Merrill et al., 1988). Zygotic mutations show their earliest effects on cell-cycle progression and patterns during mitosis 14 (this paper; V. Foe, personal communication), and many have no effect until much later in development (Lehner and O'Farrell, 1989; Baker and Gatti, submitted).

In summary, earlier studies suggested that the key regulators of cell-cycle patterns in the embryo are proteins that trigger mitosis. Moreover, they indicated that at least one of these proteins must be translated from maternal mRNA preceding each of the first 13 mitoses, and from zygotic mRNA preceding mitosis 14 and thereafter. We thought that if an embryo were to lack the gene encoding such a protein, it would traverse the first 13 mitoses by virtue of maternal message and arrest in G2 of cycle 14, when zygotic transcripts of the gene were first required. Here we show that embryos homozygous for null mutations at the *string (stg)* locus have precisely this phenotype.

We describe the cloning of *stg*, and show that it is a homolog of *cdc25*, a mitotic regulator in fission yeast (Russell and Nurse, 1986). Further, we detail the highly regulated patterns of *stg* mRNA expression during embryogenesis. An abrupt degradation of maternal *stg* mRNA during interphase 14 may be involved in terminating the early, maternally controlled nuclear divisions. More importantly, the rapidly changing patterns of zygotically expressed *stg* mRNA

predict the sequence of zygotically controlled embryonic cell divisions. This leads us to propose that *stg* mRNA levels determine the timing and location of cell divisions during embryogenesis.

Results

The *stg* Phenotype Suggests that *stg* Activity Triggers Mitosis

The eight alleles of *stg* isolated by Jürgens et al. (1984) are recessive embryonic lethals, and were originally identified because they cause a rather nonspecific reduction in the number of differentiated cuticular structures. The probable cause of this reduction was discovered by Y. N. Jan (personal communication), who noticed that *stg* embryos have a markedly reduced number of cells relative to wild-type embryos during the later stages of embryogenesis (Figure 1). This suggested that *stg* mutations caused a defect in cell proliferation.

To investigate the character of this cell-proliferation defect, we observed both live *stg* embryos under Nomarski optics, and fixed *stg* embryos that we stained to reveal the morphology of DNA, microtubules, and the nuclear envelope. We found that embryos homozygous for one the strongest alleles of *stg* (7B69) undergo the first 13 nuclear divisions with normal timing and morphology, and generate a cellular blastoderm with a wild-type number of nuclei, stg^{7B69} embryos first deviate from normal development during the early stages of gastrulation, when they fail to initiate the 14th mitosis, which normally begins at about 200 min AED (after egg deposition, 25°C). We fixed and stained embryos homozygous for the three stongest alleles of *stg* (7B69, 8A83, 7L105), and found no evidence of chromosome condensation, nuclear envelope break-down, or spindle formation between 3 and 12 hr AED (Figure 1). In contrast, most cells in wild-type embryos divide at least twice during this period (Hartenstein and Campos-Ortega, 1985). We infer that the cells formed during interphase 14 in *stg* homozygotes remain in interphase for the duration of embryogenesis.

To determine the stage of cell-cycle arrest in *stg* mutants, we measured the DNA in nuclei of stg^{7B69} embryos by scanning microdensitometry of squashed, feulgen-stained samples at about 6 hr AED. We found that these nuclei were 4C, and were thus arrested in G2 (data not shown). We also labeled DNA in stg^{7B69} and wild-type embryos by injecting BrdU during G2 of interphase 14 (240 min AED, 22°C; see Edgar and Schubiger, 1986) and allowing the embryos to develop for 3 hr (Figure 2). In wild-type embryos, which progressed through S phases 15 and 16 during the labeling period, all nuclei became heavily labeled. In *stg* embryos only the giant, polyploid nuclei of the amnioserosa were labeled. These amnioserosa nuclei normally undergo multiple rounds of DNA synthesis after mitosis 13, but never divide (Hartenstein and Campos-Ortega, 1985). Their labeling in *stg* embryos indicates that the *stg* mutation does not block the normal program of polyploidization, and implies that the DNA synthetic machinery is functional in *stg* embryos. Thus, although we know that failure to complete DNA replication can cause cell-cycle arrest in interphase 14 (Edgar and Foe, unpublished data), it seems unlikely that this is the cause of cell-cycle arrest in *stg* embryos.

stg embryos undergo a remarkably normal program of postblastoderm development despite their cell-cycle arrest. They have a normally timed series of morphogenetic movements (see Figure 1), and the 5000 cells present in *stg* homozygotes eventually express markers found in most of the differentiated tissues of wild-type embryos, which hatch with perhaps 50,000 cells (Jürgens et al., 1984; Edgar, unpublished data; V. Hartenstein, personal communication). This lack of pleiotropy suggests that *stg* activity is required rather specifically for mitotic initiation. Our preliminary analysis of some of the weaker (hypomorphic) *stg* alleles supports this conclusion. Embryos homozygous for these alleles (9A19, 4B51, 9K21) support some mitotic activity after interphase 14. The mitoses that occur seem to be delayed; they occur over a longer period of development than in wild-type embryos, but nevertheless generate fewer cells. We saw no signs of polyploidy, aneuploidy, or spindle defects in these embryos. Our observations

suggest that lowering the level of *stg* activity delays the timing of mitotic initiation without perturbing the coordination of cell-cycle events such as S phases, chromosome condensation, and spindle formation.

Cloning *stg*

stg was originally mapped to the region between bands 98A and 99A at the tip of chromosome arm 3R (Jürgens et al., 1984). We confirmed the more detailed mapping of Weigel and Jürgens (personal communication) using a series of terminal deficiencies, *stg* was uncovered by deficiencies distal to 98F, but not those distal to 99A. Thus, the region 98F–99A is required for *stg* function. We tested a P element insertion mutant at 99A, I(3)neo62 (Cooley et al., 1988), for its ability to complement the eight EMS-induced *stg* alleles of Jurgens et al. (1984). I(3)neo62 is a recessive embryonic lethal, but does not show a *stg* cuticle phenotype when homozygous. Nevertheless, it failed to complement the lethality of the strongest *stg* alleles (8A83, 7L105, 7B69), and only partially complemented the weaker *stg* alleles (13D22, 9A19, 7M53, 4B51, 9K21). Moreover, lethal transheterozygotes (stg^{7L105}/I(3)neo62) exhibited a weak *stg* cuticle phenotype.

We reverted the lethality of I(3)neo62 by transposase-mediated excision of the P element insertion (Robertson et al., 1988), and found that the reverted chromosome 3 was restored in its ability to complement stg^{7L105} and stg^{7B69}. After cloning the genomic region containing this P insertion (see below), we confirmed that the P transposon had indeed "hopped out" of the 99A insertion site in the reverted chromosome (Figure 3). In addition to I(3)neo62, three more recessive-lethal P insertions in the same 2.2 kb genomic EcoRI fragment have been isolated (I(3)neo61: Cooley et al., 1988; I(3)3A1,1(3)1D3: Y. N. Jan, personal communication; see Figure 3). These also fail to complement *stg*, and one (I(3)3A1) exhibits a strong *stg* phenotype when homozygous.

Based on these observations, we concluded that the P element insertions at 99A caused *stg* mutations, and were thus in the proximity of the *stg* gene. We used plasmid rescue of I(3)neo62 (Cooley et al., 1988), followed by chromosome walking, to isolate 33 kb of the genomic DNA surrounding the P element insertion site (Figure 3). We confirmed that we had cloned sequences from 99A by hybridizing these sequences to Drosophila polytene chromosomes (not shown).

DNA fragments from this 33 kb genomic region were used to probe developmental Northern blots, and we found at least two transcription units in the cloned region (Figure 3). The transcribed region nearest the P element insertion site (less than 1 kb downstream) produces mRNAs of approximately 2.8 and 3.0 kb. The expression of these transcripts is as expected of a product involved in cell division: they are abundant during periods of much cell division (mitoses 1–13 and mitoses 14–16) and scarce during periods of little cell division (G2 of cycle 14 and postmitosis 16). The other RNAs transcribed from regions not adjacent to the P insertion site do not follow this profile (Figure 3). This suggests that the transcription unit adjacent to the P insertion site encodes the *stg* product, a conclusion that was strongly supported by further analysis in which we determined the sequence of mRNAs from this region and detailed their spatial patterns of expression (see below). Moreover, we found that embryos homozygous for the P element insertion I(3)3A1, a strong allele of *stg*, failed to express detectable amounts of the putative *stg* transcripts during postblastoderm development. This was determined by in situ hybridization of a *stg* cDNA probe (see below) to embryos derived from I(3)3A1/TM3 parents (data not shown).

stg Is Homologous to *cdc25* of S. pombe

Using genomic DNA probes, we isolated cDNAs corresponding to the putative *stg* mRNAs. We sequenced a 2308 base *stg* cDNA and found a single long open reading frame (Figure 4).

Searches of the Dayhoff protein sequence data base revealed that the predicted *stg* protein of 479 amino acids includes a C-terminal region of 187 amino acids that is 34% identical to the C-terminal portion of the *cdc25* protein of the yeast S. pombe (Figure 5). The molecular function of *cdc25* is not known, but genetic experiments indicate that it plays a role in cell-cycle regulation similar to *stg*: in a wild-type background, *cdc25* is required for progression from G2 to mitosis, and when overexpressed it causes premature initiation of mitosis (Fantes, 1981;Russell and Nurse, 1986). In addition to the sequence homology, *stg* cDNA clones can complement the *cdc25–22* temperature-sensitive mutation in S. pombe, showing that *stg* is a functional *cdc25* homolog (P. Russell, personal communication). Another functional homolog of *cdc25*, *MIH1*, has recently been found in S. cerevisiae (Russell et al., 1989). *MIH1* shares sequence homology with *cdc25* in the same regions that *stg* does (Figure 5).

stg mRNA Expression Predicts the Sequence of Embryonic Cell Divisions

The phenotype of *stg* mutants shows that *stg* gene expression is required for the initiation of mitosis 14. Thus, in theory, differential expression of *stg* prior to mitosis 14 could cause the complex spatio–temporal pattern of mitotic initiation seen at this stage of development. To test this possibility, we analyzed the expression of *stg* mRNA during embryonic development by in situ hybridization of a *stg* cDNA probe to whole and sectioned embryos (Figures 6 and 7).

The Drosophila egg contains a large amount of maternal *stg* mRNA that is distributed uniformly throughout the yolk and cytoplasm (data not shown, but see Figures 3e and 3f). We know this RNA is maternal because it is present in unfertilized eggs, and because our studies with transcription and protein synthesis inhibitors indicate that *stg* transcription is negligible through cycle 13 (data not shown, but see Edgar et al., 1986b, and Weir et al., 1988, for examples of this kind of study). Maternal *stg* mRNA persists at a constant level from fertilization through cycle 13, and is degraded to a level undetectable by in situ hybridization during the first 20–30 min of interphase 14. Although *stg* has not yet been tested for a maternal effect, it seems likely that *stg* protein produced from maternal mRNA is required for the early, rapid nuclear cycles. If this is the case, the abrupt degradation of maternal *stg* mRNA after mitosis 13 could cause the termination of these cycles.

Zygotically synthesized *stg* mRNA begins to accumulate in the latter half of interphase 14, 25–35 min before the first cells enter mitosis 14. Accumulation is limited to cells that are destined to divide, and occurs with a temporal sequence nearly identical to, but preceding, the sequence of mitoses (Figures 6 and 7). The spatio–temporal pattern of mitosis 14 has been studied in detail by Foe (1989), who constructed an atlas of mitotic domains. She defines a mitotic domain as a group of cells that divide together, with timing distinct from their neighbors, and designates these domains with numbers indicating their relative order of entry into mitosis. The earliest zygotic *stg* expression is in a wide ribbon of cells along the ventral surface of the blastoderm that will invaginate to form the mesoderm (Figure 6A). This region corresponds to mitotic domain 10. Several minutes later, as the cephalic furrow begins to form, expression begins in a set of bilaterally symmetric stripes and spots in the head region (mitotic domains 1–3, 5–8), and the tail (mitotic domain 4; Figure 6B). Following this, as the first mitoses occur in the head, *stg* expression ensues in the dorsolateral regions, which correspond to mitotic domain 11. Expression in domain 11 initiates in five distinct spots (Figure 6C) and then spreads to fill the entire domain (Figure 6D). Twenty-five to thirty-five minutes after expression is first observed, mitoses begin to traverse the domain in a similar manner, initiating at five centers and spreading to the borders of the domain (Foe, 1989). At about the same time as expression in domain 11 becomes detectable, expression begins along the margin of the ventral furrow (mitotic domain 14; Figure 6E), and in expanded regions of the head (mitotic domains 9 and 15; Figure 7A) and tail (mitotic domains 12 and 13; Figure 6D). Just after this, expression begins in a series of segmentally repeated spots in the abdominal ventral ectoderm (mitotic domains 16 and 17,

Figure 6E). In all of these cases we are able to correlate the regions of *stg* expression with mitotic domains using both the atlas constructed by Foe (1989) and the distribution of mitotic figures visible in our in situ preparations. Moreover, minor variations in the shapes and symmetry of the mitotic domains seen between different embryos are also reflected in the *stg* RNA patterns.

Our in situ preparations allowed us to assess, albeit crudely, relative levels of transcript in different regions of the embryo. We found that the sequence with which cells achieve high levels of *stg* RNA and the sequence of mitotic initiation are highly correlated (Figure 7). This can be seen within single domains, such as domain 11, where high levels of *stg* RNA are reached earliest in the five origins of mitosis mentioned above (Figures 6C and 6D). It can also be seen between domains; for example, although zygotic *stg* RNA is detected first in mitotic domain 10 (Figure 6A), accumulation proceeds more rapidly in domains 1–9, which initiate expression slightly later but nevertheless divide earlier (Figure 6B). These observations suggest that the level of accumulated *stg* activity determines the timing of mitosis. This notion is supported by our observation that the reduction of *stg* activity by hypomorphic *stg* mutations delays the timing of mitosis.

After mitosis, *stg* RNA disappears from most of the early dividing domains, and begins to accumulate in the ventral ectoderm, where many of the later dividing domains (21, 22,24,25, M, and N) are located (Figures 6F and 6G). During mitotic cycles 15 and 16, *stg* RNA expression recurs in a series of rapidly changing and increasingly complex patterns (data not shown). These patterns correlate well with maps of the mitotic pattern during these stages (Hartenstein and Campos-Ortega, 1985; Foe, personal communication), and with the distribution of mitotic figures in our in situ preparations, but we have not yet attempted a detailed analysis. Most cell lineages stop dividing after the 16th mitosis, during germ-band shortening. At this stage, *stg* RNA expression also ceases in most of the embryo. Cell proliferation continues primarily along the ventral surface of the nerve cord, in the brain cortex, and in the peripheral nervous system, where *stg* mRNA expression also continues (data not shown).

Discussion

The *stg* locus encodes an evolutionarily conserved regulator of mitotic initiation that appears to play two roles in regulating the embryonic cell cycles of Drosophila. First, the abrupt degradation of maternal *stg* mRNA just after the last maternally controlled mitosis may terminate the maternal mitotic program. Second, the correspondence of zygotic *stg* expression with the patterns of zygotically controlled mitoses suggests that regulated *stg* expresson governs the patterns of cell division during postblastoderm embryogenesis.

What Is *stg*?

Embryos lacking zygotic *stg* activity undergo cell-cycle arrest in G2 of interphase 14, just prior to the first zygotically controlled mitosis. This effect is highly specific; other aspects of development, such as cell movements and differentiation, proceed for many hours after the cell-cycle block. When *stg* activity is reduced by hypomorphic mutations, morphologically normal mitoses occur but their number is reduced and their timing delayed. These facts suggest that the *stg* product specifically catalyzes the initiation of mitosis, possibly in a level-dependent fashion. Since mitotic initiation seems to be the primary point of regulation in the early embryonic cell cycles (see Introduction), *stg* probably regulates not only mitosis, but cell-cycle progression in general.

The finding that *stg* is a structural and functional homolog of *cdc25* from S. pombe allows a more specific speculation about its activity. Based on genetic studies, Russell and Nurse

(1986) proposed that *cdc25* is a level-dependent activator of another factor required to initiate mitosis, the *cdc2* protein kinase. *cdc2* encodes a component of MPF (mitosis promoting factor), an activity that is ubiquitous in proliferating eukaryotic cells (Dunphy and Newport, 1988b; Gautier et al., 1988). In both cultured human cells and Xenopus embryos, *cdc2* protein is present during all phases of the cell cycle, but its kinase activity is activated prior to each mitosis (Draetta and Beach, 1988; Arion et al., 1988; see also Cyert and Kirschner, 1988; Dunphy and Newport, 1988a). This activation is presumed to trigger a cascade of phosphorylation events leading to nuclear envelope breakdown, chromosome condensation, spindle formation, and other mitotic functions (Newport and Kirschner, 1984; Karsenti et al., 1987; see Fantes, 1988, Lee and Nurse, 1988, and Dunphy and Newport, 1988c, for reviews). This set of relationships suggests that *stg* may trigger mitosis by activating a Drosophila *cdc2* homolog.

Does *stg* Control the Developmental Pattern of Mitoses?

A simple way to regulate cell divisions differentially during development would be to express all but one of the required factors constitutively, and to then modulate expression of the single remaining, rate-limiting factor. Our findings are consistent with this type of regulation, and suggest that *stg* mRNA is the rate-limiting factor whose expression governs mitotic patterns after interphase 14. The most suggestive of these findings are first, that *stg* mRNA is expressed in a spatio–temporal pattern that anticipates the mitotic pattern, and second, that the *stg* gene is required zygotically for initiation of the first patterned mitosis. Since cell-cycle arrest occurs earlier in *stg* mutants than in any other characterized zygotic mutant, it seems likely that maternal supplies of other cell-cycle factors persist past the time when *stg* becomes required. The work of Lehner and O'Farrell (1989) on Drosophila cyclin A provides a clear example of a product that is required for mitosis yet seems not to be rate-limiting during the first zygotically controlled divisions. In contrast to *stg*, cyclin A derived from maternal mRNA is sufficient to support divisions through mitosis 15, and the level of cyclin A protein has little influence on the timing of mitoses.

We have demonstrated directly only that *stg* is required for mitosis 14, but our observations of mitotic patterns in hypomorphic and temperature-sensitive *stg* mutants suggest that *stg* is required for subsequent embryonic mitoses (Edgar, unpublished data). In addition, clonal analysis has indicated that *stg* is required for cell divisions in the imaginal discs during metamorphosis (Terle and Saint, personal communication). Although such observations do not address whether *stg* continues to be rate-limiting during later mitoses, the continued correlation of *stg* expression with mitotic patterns suggests that *stg* expression could determine the timing of all the postblastoderm divisions.

How Is *stg* Expression Controlled?

Perhaps our most significant finding is that the pattern of embryonic cell divisions may be predicted from the expression pattern of *stg* messenger RNA (Figure 7). This implies that the mitotic pattern may be controlled through differential rates of *stg* transcription and/or RNA degradation. While we know little about RNA degradation in Drosophila, recent studies have defined a plethora of factors involved in generating complex spatio–temporal patterns of transcription during embryogenesis (see Ingham, 1988, for review). These factors are encoded by the "selector" genes that set up patterns and determine cell identities in the embryo. To date, most of the selector genes studied at the molecular level encode DNA binding proteins of the zinc finger or homeodomain types that reside in the nucleus, and are widely believed to be transcription factors (see Gaul and Jäckle, 1987;Scott et al., 1989). This is fitting, since it has long been thought that selector genes determined cell fates by modulating the expression of "cytodifferentiation" genes encoding products directly responsible for cell structure, movement, and division (Garcia-Bellido, 1975). Our understanding of *stg*'s function clearly classifies it as a cytodifferentiation gene, and thus as a likely target of selector-gene regulation.

There are more compelling reasons than theory, however, to believe that *stg* is a selector-gene target. One is that the selector-gene expression patterns exhibit uncanny similarities to the *stg* expression patterns. Preceding mitosis 14, *stg* expression along the dorsoventral axis of the embryo is broken up into at least six distinct patterns that fall into the six dorsoventral domains defined by selector genes such as *zerknüllt*, *twist*, and those of the *spitz* group (Ingham, 1988; Mayer and Nüsslein-Volhard, 1988). Along the anteroposterior axis, *stg* expression is divided into different patterns in the head, thorax, abdomen, and tail, regions that are determined by differential expression of selector genes of the gap and homeotic classes (Gaul and Jäckle, 1987; Gehring, 1987). Within these regions, *stg* expression occurs in reiterated patterns with double- and single-segment periodicity that resembles pair-rule and segment-polarity gene expression patterns (Ingham, 1988).

In theory, the various selector-gene expression patterns subdivide the embryo into enough uniquely specified domains to account for virtually all aspects of *stg* expression during cycle 14. Moreover, the patterns of mitosis 14 are altered in predictable ways in many selector-gene mutants (Foe, personal communication). We expect that the altered patterns of mitosis in these mutants will be correlated with altered patterns of *stg* expression. Accordingly, we would like to propose that *stg* activity, and thus the mitotic pattern, is regulated at the transcriptional level by a variety of selector-gene products. Much of this regulation may be indirect, but the relative timing of selector-gene and *stg* expression suggests that direct interactions, perhaps using combinations of selector-gene encoded transcription factors, are involved.

Is Mitosis Important?

One higher order question that the *stg* mutations and clones will help us address is the relationship of cell-division patterns to other developmental processes. Cell division is clearly essential to generate the correct number of cells in different tissues and organs during development, and also plays a role, in conjunction with control of the orientation of division, in forming morphological structure (see Foe, 1989). It has also often been proposed that cell-cycle functions might somehow feed back on states of gene expression, thereby influencing determination and differentiation during development (Holtzer et al., 1975; Edgar and McGhee, 1988). Despite these expectations, the surprising degree of differentiation that occurs in *stg* mutants, which lack all postblastoderm cell divisions, indicates that the cell-division program in Drosophila may have little influence on morphogenetic movements, cell determination, or differentiation. Instead, different aspects of cell fate such as mitotic timing, movement, and structural differentiation seem to be regulated independently. Since all of these functions are directed by selector-gene expression, it would seem that the selector genes regulate many different types of target genes independently.

Experimental Procedures

Mapping and Reversion of *stg*

The cytological position of *stg* was confirmed by crossing *stg* ^{7B69}/TM3 or *stg* ^{481}/TM3 to T(Y:3)R78/TM6, T(Y:3)J151/TM6, T(Y:3)B152/TM6 (breakpoints in 98F), and T(Y:3)In(3R)B172/TM6 (relevant breakpoint in 99A). The lethal progeny of these crosses were scored for the *stg* cuticle phenotype. Only T(Y:3)In(3R)B172/TM6 did not give *stg* embryos, indicating *stg* is proximal to 99A.

I(3)neo62 was reverted by crossing I(3)neo62 r e mwh/TM3 Sb e flies to Δ2–3 Sb/TM6 Ubx e flies that carry a stable transposase source on chromosome 3 (Δ2–3; Robertson et al., 1988). Dysgenic male progeny of the genotype I(3)neo62 r e mwh/Δ2–3 Sb were then mated to I(3)neo62 r e mwh/TM3 Sb e females. Homozygous Sb^{+} r e mwh progeny occurred at a frequency of about 2%–4%. These presumably heterozygous revertants of the genotype I(3)

neo62 r e mwh/neo62^{R} r e mwh were crossed to *stg*^{7B69} e/TM3 Sb e flies to test for *stg* complementation. Sb^{+} e flies, presumably of the genotype *stg*^{7B69} e/neo62^{R} r e mwh occured at a frequency of 43%. These were then mated to each other, and homozygous r e mwh progeny were picked and mated to each other to establish the homozygous revertant lines whose DNA was used in Southern analysis (Figure 3).

Cloning and Blot Hybridizations

Plasmid rescue was carried out according to Cooley et al. (1988) using genomic DNA isolated from I(3)neo61/TM3 or I(3)neo62/TM3 flies cut with SaII, EcoRI, or BamHI. Similar flanking fragments were recovered from both strains. Genomic DNA clones were isolated from a λ-dash library (a gift from L. and Y. N. Jan), and cDNA clones were isolated from the L. Kauvar λgt10 library according to standard protocols, with conditions as described in Lehner and O'Farrell (1989). DNA preparations for Southern blots were carried out as in Lehner and O'Farrell (1989). Northern blots were done as described in Edgar et al. (1986b), using total RNA from 100 individually staged embryos per lane, formaldehyde-agarose gels, and Hybond-N nylon filters (Amersham). Probes were made from gel-isolated restriction fragments by the random primer method (Hodgson and Fisk, 1987).

In Situ Hybridizations

Whole-mount hybridizations were done as follows. Embryos were dechorionated in 50% bleach for 2 min, fixed for 20 min in a two-phase mixture of heptane over PBS, 50 mM EGTA, and 10% formaldehyde, and devitellinized by replacing the aqueous fixative with absolute methanol and shaking vigorously. After two rinses in methanol, they were rinsed twice in 95% ethanol and stored in 95% ethanol at −20°C for 1–20 days. The embryos were rehydrated by two rinses in PBS containing 0.05% Triton X-100 (PTx), and acetylated by rinsing for 5 min in 1 × PBS, 0.1 M triethanolamine (pH 7.8), 0.5% acetic anhydride (added just before the embryos). They were then rinsed twice in PTx, and pre-hybridized for 1 hr at 50°C in 50 μl of a solution containing 50% de-ionized formamide, 0.6 M NaCl, 10 mM Tris 7.5, 1 mM EDTA, 1% SDS, 1× Denhardt's, 10% PEG 8000, 0.03% Triton X-100, 0.25 mg\ml E. coli tRNA. Hybridizations were done for 12 hr at 50°C in 50 μl of the above solution containing 10^{7} cpm of antisense RNA probe. We snythesized antisense RNA probes with T7 polymerase from a cDNA template of 1.3 kb from the 5′ region of the *stg* message (pC8). Probes were labeled with [^{35}S]UTP or [^{3}H]ATP, GTP, and UTP of the highest specific activity available (Amersham). After probe synthesis, the DNA template was removed with DNAase, and the probes were base-hydrolyzed to a mean length of about 100 bases by incubation in 40 mM $NaHCO_3$, 60 mM Na_2CO_3 for 90 min at 60°C. After hybridization, the embryos were rinsed three times in PBS, and incubated for 60 min at 37°C in 100 μg/ml RNAase A, 0.5 M NaCl, 10 mM Tris 7.5. They were then washed three times in 1× SSPE, 50% formamide, 0.05% SDS, 0.05% Triton X-100, and three more times in 0.1 × SSPE, 0.05% SDS, 0.05% Triton X-100. Washes were done in 800 μl, for 30 min, at 50°C. Finally, the embryos were rinsed in PTx. Ten to twenty embryos were mounted with even spacing onto a formaldehyde-activated TESPA-coated slide (Berger, 1986) in about 30 μl of PTx. A siliconized 22 mm^{2} cover slip was applied, and as much liquid as possible was wicked away by applying gentle pressure and touching a filter paper to the edges of the cover slip. This flattened the embryos, allowing an even application of the photographic emulsion. The cover slip was then removed by rinsing the slide in a bath of 95% ethanol, and the slide was air dried. We applied 66% Kodak NTB-2 nuclear track emulsion by standard methods, and exposed the slides for 6 days (^{35}S probes) or 5 months (^{3}H probes). After developing the slides, the embryos were stained in 10 μg/ml Hoechst 33258 for 3 min, rinsed in water for 15 min, air dried, and mounted in a mixture of Canada balsam and methyl salycilate that was the consistency of maple syrup.

Acknowledgments

We are indebted to C. Nüsslein-Volhard, L. Cooley, and Y. N. Jan for *stg* mutants, to D. Weigel, G. Jürgens, R. Terle, and R. Saint for information about the map position of *stg*, and to S. DiNardo and C. Lehner for copious technical advice. We would especially like to thank Steve DiNardo for bringing I(3)neo62 to our attention, Paul Russell for testing *stg* in S. pombe, and Victoria Foe for unpublished data maps of the mitotic pattern. Jill Heemskerk-Jongens, Delia Lakich, Christian Lehner, and Maria Leptin provided valuable criticism of the manuscript. This work was supported by a National Science Foundation grant to P. O'F. and an American Cancer Society Postdoctoral Fellowship to B. A. E.

References

Arion D, Meijer L, Brizuela L, Beach D. *cdc2* is a component of the M phase–specific histone H1 kinase: evidence for identity with MPF. Cell 1988;55:371–378. [PubMed: 2844417]

Berger C. In situ hybridization of immunoglobulin-specific RNA in single cells of the B lymphocyte lineage with radiolabeled DNA probes. EMBO J 1986;5:85–93. [PubMed: 3007120]

Blow JJ, Laskey RA. A role for the nuclear envelope in controlling DNA replication within the cell cycle. Nature 1988;332:546–548. [PubMed: 3357511]

Blumenthal AB, Kriegstein HJ, Hogness DS. The units of DNA replication in Drosophila melanogaster chromosomes. Cold Spring Harbor Symp Quant Biol 1974;38:205–223. [PubMed: 4208784]

Cavener DR. Comparison of the consensus sequence flanking translational start sites in Drosophila and vertebrates. Nucl Acids Res 1987;15:1353–1361. [PubMed: 3822832]

Cooley L, Kelley R, Spradling A. Insertional mutagenesis of the Drosophila genome with single P elements. Science 1988;239:1121–1128. [PubMed: 2830671]

Cyert MS, Kirschner MW. Regulation of MPF activity in vitro. Cell 1988;53:185–195. [PubMed: 2834064]

Draetta G, Beach D. Activation of *cdc2* protein kinase during mitosis in human cells: cell cycle–dependent phosporylation and subunit rearrangement. Cell 1988;54:17–26. [PubMed: 3289755]

Dunphy WG, Newport JW. Mitosis-inducing factors are present in a latent form during interphase in the Xenopus embryo. J Cell Biol 1988a;106:2047–2056. [PubMed: 3290226]

Dunphy WG, Newport JW. The Xenopus *cdc2* protein is a component of MPF, a cytoplasmic regulator of mitosis. Cell 1988b;54:423–431. [PubMed: 3293802]

Dunphy WG, Newport JW. Unraveling of mitotic control mechanisms. Cell 1988c;55:925–928. [PubMed: 3060263]

Edgar LG, McGhee JD. DNA synthesis and the control of embryonic gene expression in Caenorhabditis elegans. Cell 1988;53:589–599. [PubMed: 3131016]

Edgar BA, Schubiger G. Parameters controlling transcriptional activation during early Drosophila development. Cell 1986;44:871–877. [PubMed: 2420468]

Edgar BA, Kiehle CP, Schubiger G. Cell cycle control by the nucleo-cytoplasmic ratio in early Drosophila development. Cell 1986a;44:365–372. [PubMed: 3080248]

Edgar BA, Weir MP, Schubiger G, Kornberg T. Repression and turnover pattern fushi tarazu RNA in the early Drosophila embryo. Cell 1986b;47:747–754. [PubMed: 3096577]

Fantes PA. Isolation of cell size mutants of a fission yeast by a new selective method: characterization of mutants and implications for division control mechanisms. J Bacteriol 1981;146:746–754. [PubMed: 7217015]

Fantes P. Intersecting cell cycles. Trends Genet 1988;4:275–276. [PubMed: 3076287]

Foe VE. Mitotic domains reveal early commitment of cells in Drosophila embryos. Development. 1989in press

Foe VE, Alberts BM. Studies of nuclear and cytoplasmic behavior during the five mitotic cycles that precede gastrulation in Drosophila embryogenesis. J Cell Sci 1983;61:31–70. [PubMed: 6411748]

Garcia-Bellido, A. Genetic control of wing disc development in Drosophila. Cell Patterning, Volume 29, CIBA Symposium; Amsterdam: Elsevier; 1975. p. 161-183.

Gaul U, Jäckle H. How to fill a gap in the Drosophila embryo. Trends Genet 1987;3:127–131.

Gautier J, Norbury C, Lohka M, Nurse P, Maller J. Purified maturation-promoting factor contains the product of a Xenopus homolog of the fission yeast cell cycle control gene *cdc2*$^{+}$ Cell 1988;54:433–439. [PubMed: 3293803]

Gehring WJ. Homeo boxes in the study of development. Science 1987;236:1245–1252. [PubMed: 2884726]

Gutzeit HO. Expression of the zygotic genome in blastoderm stage embryos of Drosophila: analysis of a specific protein. Roux's Arch Dev Biol 1980;188:153–156.

Harland RM, Laskey RA. Regulated replication of DNA microinjected into eggs of Xenopus laevis. Cell 1980;21:761–771. [PubMed: 6254667]

Hartenstein V, Campos-Ortega JA. Fate-mapping in wild-type Drosophila melanogaster I. The spatio–temporal pattern of embryonic cell divisions. Roux's Arch Dev Biol 1985;194:181–195.

Hodgson CP, Fisk RZ. Hybridization probe size control: optimized "oligolabeling". Nucl Acids Res 1987;15:6295. [PubMed: 3627988]

Holtzer H, Rubinstein N, Fellini S, Yeoh G, Chi J, Birnbaum J, Okayama M. Lineages, quantal cell cycles, and the generation of cell diversity. Quarterly Rev Biophys 1975;8:523–557.

Ingham PW. The molecular genetics of embryonic pattern formation in Drosophila. Nature 1988;335:25–33. [PubMed: 2901040]

Jürgens G, Wieschaus E, Nüsslein-Volhard C. Mutations affecting the pattern of the larval cuticle in Drosophila melanogaster. II Zygotic loci on the third chromosome. Roux's Arch Dev Biol 1984;193:283–295.

Karsenti E, Bravo R, Kirschner M. Phosporylation changes associated with the early cell cycle in Xenopus eggs. Dev Biol 1987;119:442–453. [PubMed: 3803713]

Lee M, Nurse P. Cell cycle control genes in fission yeast and mammalian cells. Trends Genet 1988;4:287–290. [PubMed: 3076289]

Lehner CF, O'Farrell PH. Expression and function of Drosophila cyclin A during embryonic cell cycle progression. Cell 1989;56:957–968. [PubMed: 2564316]

Mayer U, Nüsslein-Volhard C. A group of genes required for pattern formation in the ventral ectoderm of the Drosophila embryo. Genes Dev 1988;2:1496–1511. [PubMed: 3209069]

McKnight SL, Miller OL Jr. Electron microscopic analysis of chromatin replication in the cellular blastoderm Drosophila melanogaster embryo. Cell 1977;12:795–804. [PubMed: 411576]

Merrill PT, Sweeton D, Wieschaus E. Requirements for autosomal gene activity during precellular stages of Drosophila melanogaster. Development 1988;104:495–503. [PubMed: 3151484]

Mita I. Studies on factors affecting the timing of early morphogenetic events during starfish embryogenesis. J Exp Zool 1983;225:293–299.

Murray AW. A cycle is a cycle is a cycle. Nature 1987;327:14–15. [PubMed: 3574461]

Newport J, Kirschner M. A major developmental transition in early Xenopus embryos: I. Characterization and timing of cellular changes at the midblastula stage. Cell 1982;30:675–686. [PubMed: 6183003]

Newport JW, Kirschner MW. Regulation of the cell cycle during early Xenopus development. Cell 1984;37:731–742. [PubMed: 6378387]

Olszanska B, Kludkiewicz B, Lassota Z. Transcription and polyadenylation processes during early development of quail embryo. J Embryol Exp Morph 1984;79:11–24. [PubMed: 6201580]

Rabinowitz M. Studies on the cytology and early embryology of the egg of Drosophila melanogaster. J Morph 1941;69:1–49.

Robertson HM, Preston CR, Phillis RW, Johnson Sclitz D, Benz WK, Engels WR. A stable source of P element transposase in Drosophila melanogaster. Genetics 1988;118:461–470. [PubMed: 2835286]

Russell P, Nurse P. *cdc25*$^{+}$ functions as an inducer in the mitotic control of fission yeast. Cell 1986;45:145–153. [PubMed: 3955656]

Russell P, Moreno S, Reed SI. Conservation of mitotic controls in fission and budding yeasts. Cell. 1989in press

Schubiger M, Palka J. Changing spatial patterns of DNA replication in the developing wing of Drosophila. Dev Biol 1987;123:145–153. [PubMed: 3622926]

Scott MP, Tamkun JW, Hartzell GW. The structure and function of the homeodomain. BBA Rev Cancer. 1989in press

Steller H, Pirotta V. A transposable P vector that confers selectable G418 resistance to Drosophila larvae. EMBO J 1985;4:167–171. [PubMed: 16453599]

Sulston JE, Schierenberg E, White JC, Thompson JN. The embryonic lineage of the nematode Caenorhabditis elegans. Dev Biol 1983;100:64–119. [PubMed: 6684600]

Wieschaus E, Sweeton D. Requirements for X-linked zygotic gene activity during cellularization of early Drosophila embryos. Development 1988;104:483–493. [PubMed: 3256473]

Weir MP, Edgar BA, Kornberg T, Schubiger G. Spatial regulation of engrailed expression in the Drosophila embryo. Genes Dev 1988;2:1194–1203. [PubMed: 2461329]

Weisblat DA, Harper G, Stent GS, Sawyer RT. Embryonic cell lineages in the nervous system of the glossiphoniid leech Helobdella triserialis. Dev Biol 1980;76:58–78. [PubMed: 7380099]

Zalokar M, Audit C, Erk I. Developmental defects of female-sterile mutants of Drosphila melanogaster. Dev Biol 1975;47:419–432. [PubMed: 812739]

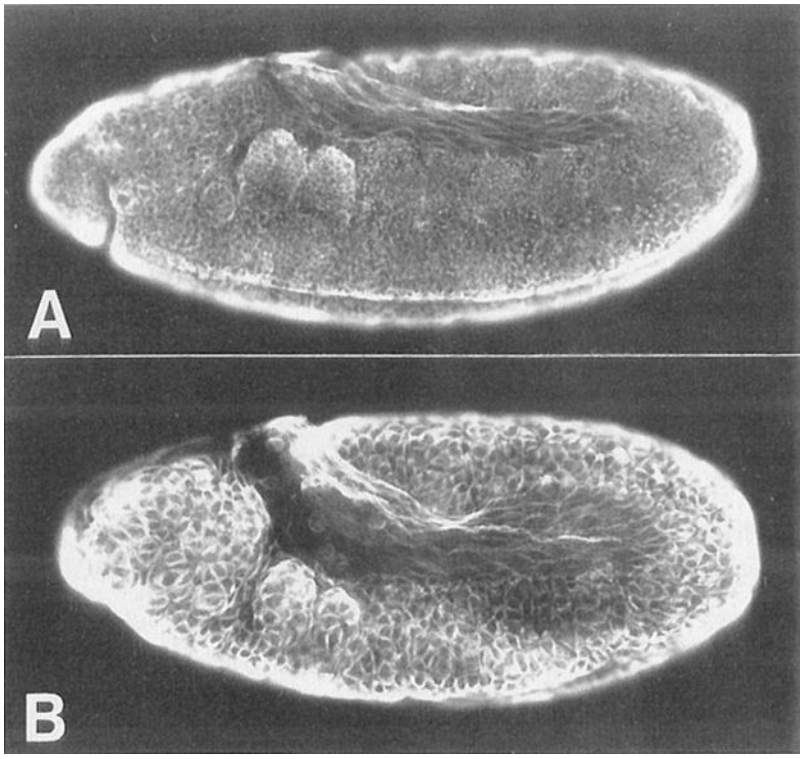

Figure 1. Wild-Type (A) and *stg* (B) Embryos at about 6 Hr AED, Stained with Anti-Tubulin Antibodies

Anterior is to the left and dorsal is up. Tubulin outlines the cells during interphase, and forms spindles (which appear as bright dots) during mitosis. Note that the *stg* embryo has many fewer cells than the wild-type embryo. The wild-type embryo is undergoing mitosis 15, whereas the *stg* embryo is arrested in interphase 14. Other morphological features, such as the extended germ band, gnathal lobes, and amnioserosa, are similar in both embryos.

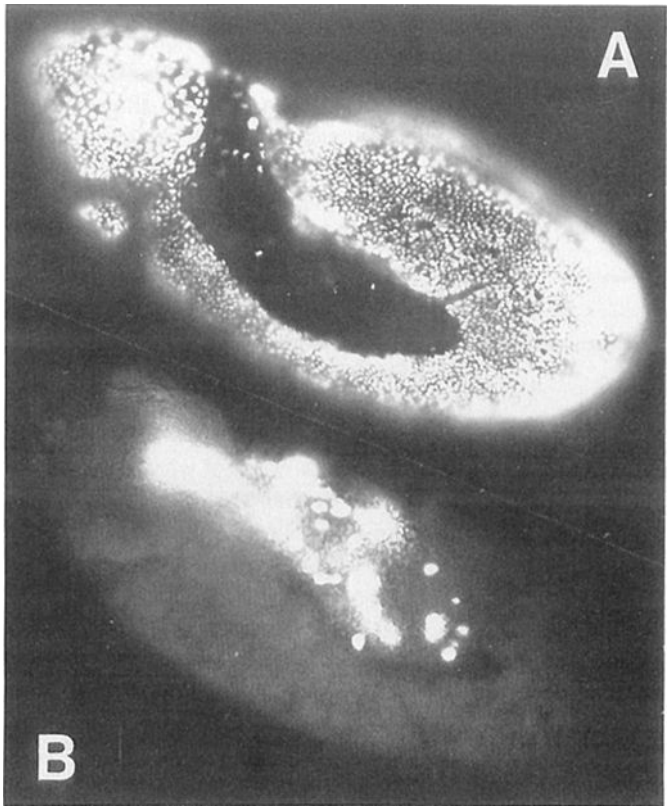

Figure 2. DNA Synthesis in (A) Wild-Type and (B) *stg*^{7B69} Embryos

Anterior is to the left and dorsal up. We injected these embryos with 50 mM BrdU (pH 9) during G2 of cycle 14, allowed them to develop for 3 hr, and then fixed them. BrdU-labeled DNA was detected by indirect immunofluorescence (Schubiger and Palka, 1987). All nuclei in the wild-type embryo are labeled, whereas only the polyploid nuclei of the amnioserosa are labeled in the *stg*^{7B69} embryo. In the wild-type embryo (A), the amnioserosa nuclei are polyploid, but are not heavily labeled. This is probably due to depletion of the injected BrdU prior to polyploidization.

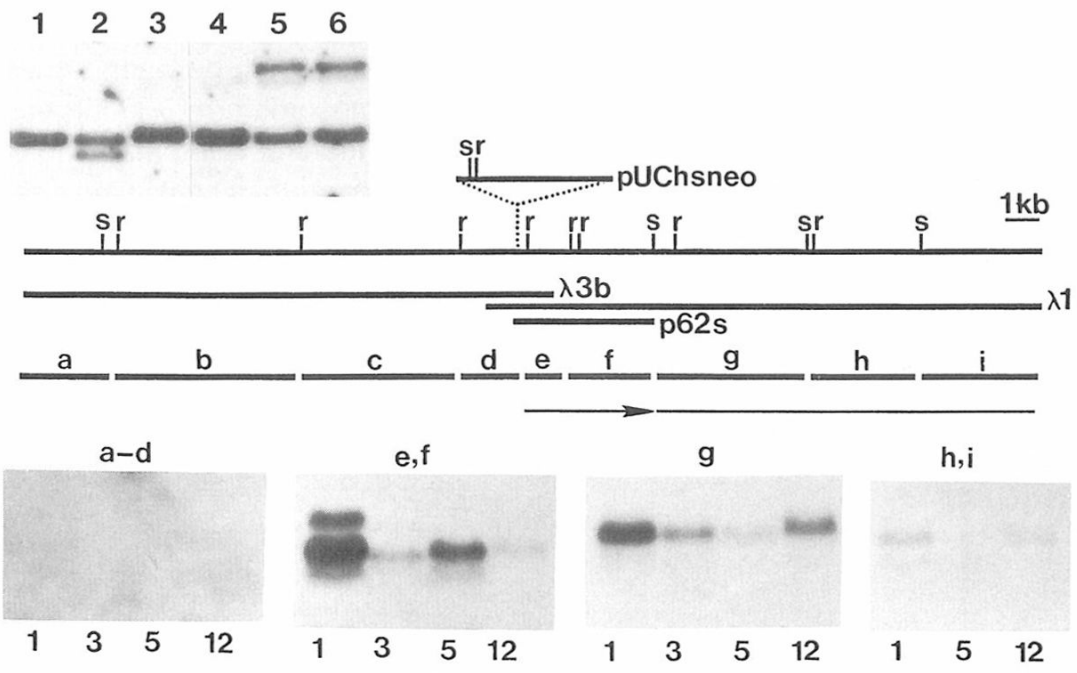

Figure 3. Cloning of the *stg* Locus

The figure shows a restriction map of the 33 kb genomic region that contains the *stg* locus, with EcoRI (r) and SaII (s) sites indicated. The insertion site of the *P* element (pUChsneo; Steller and Pirotta, 1985) in *stg* mutants I(3)-neo61 and I(3)neo62 is indicated above the map. We isolated 4.5 kb of DNA flanking these insertions by plasmid rescue (p62s) and used this to isolate genomic clones (λ1, λ3b) from a lambda library.

The entire region was fragmented into nine contiguous pieces (a–i), and the isolated fragments were used to probe developmental Northern blots, examples of which are shown below the map. Probes a–d detected no transcripts, probes *e* and f detected transcripts of 2.8 and 3.0 kb, probe g detected a 2.9 kb transcript, and probes h and i detected transcripts of 2.9 and 2.7 kb. The inferred transcribed regions are indicated by thin lines below the probe fragments, and the direction of transcription of the presumed *stg* transcripts is indicated with an arrow. Numbers below the blots indicate hr AED at 22°C. One-hour embryos (1) are rapidly cleaving, 3 hr embryos (3) are in interphase 14, 5 hr embryos (5) are undergoing mitoses 14 and 15, and 12 hr embryos (12) have only a few mitoses, mainly in the nervous system.

Above the restriction map we show a Southern blot of genomic DNA from the various P element mutants and revertants, cut with EcoRI and hybridized with probe d, a 2.2 kb genomic EcoRI fragment. Numbers above the gel panel indicate genotypes: (1) I(3)neo31/TM3 (a P element insertion at a different site, this is a control); (2) I(3)neo62/TM3; (3) revertant $neo62^{R2}/neo62^{R2}$; (4) revertant $neo62^{R5}/neo62^{R5}$; (5) I(3)3A1/TM3; (6) I(3)1D3/TM3. Sizes of the bands detected are 3.6, 2.2, and 2.1 kb, top to bottom. The wild-type band is 2.2 kb (lane 1). In each of the P element insertion mutants, this band is altered in size (lanes 2, 5, 6), and in the P element revertants it is restored to approximately the wild-type size (lanes 3 and 4).

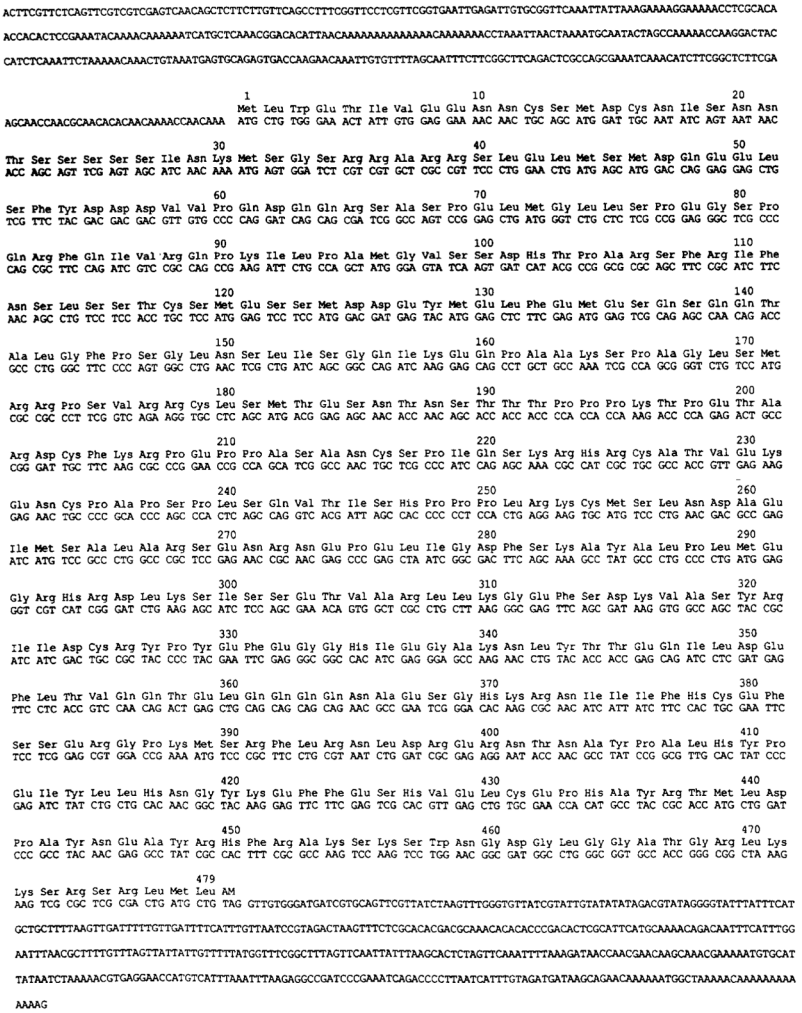

Figure 4. Nucleotide and Predicted Amino Acid Sequence of a 2308 Base *stg* cDNA That Is Homologous to Genomic Fragments e and f (Figure 3)

The translation initiation site was chosen to maximize the length of the open reading frame. Both this site and one at position 31 match the consensus sequence for translation initiation sites in Drosophila (Cavener, 1987).

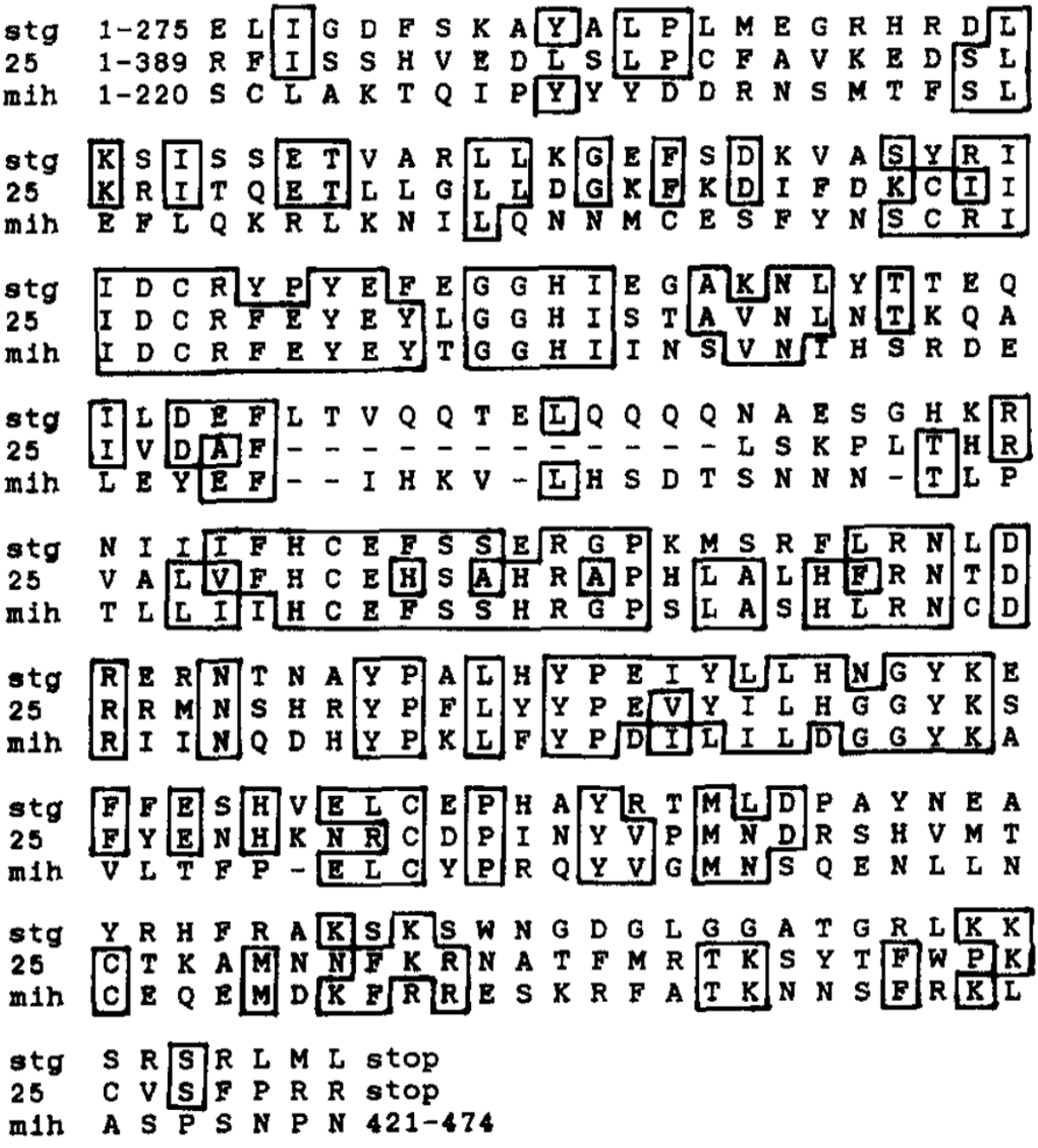

Figure 5. The Predicted Amino Acid Sequence of *stg* Is Homologous to *cdc25* of S. pombe (25) and *MIH1* of S. cerevisiae (mih)

The C-terminal regions of the three sequences are aligned, and identical amino acids are boxed. The three sequences are approximately 35% identical in a 187 amino acid stretch included in the figure. We found no significant homologies in the N-terminal regions of these proteins.

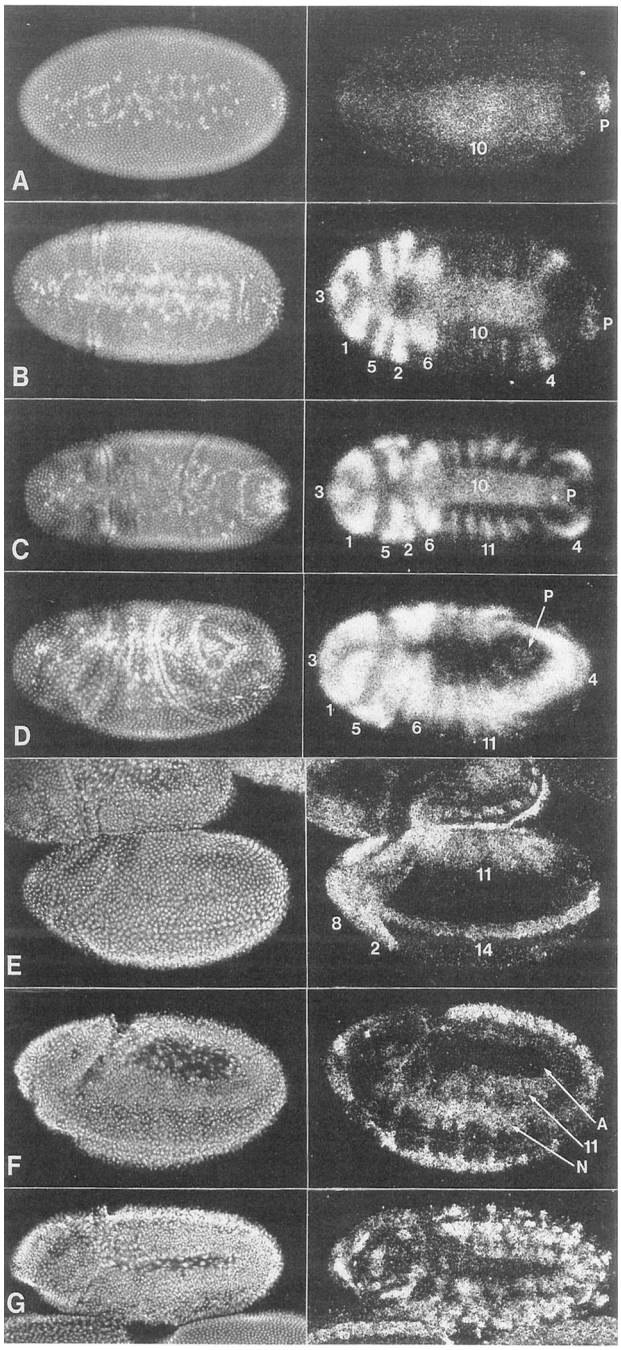

Figure 6. A Temporal Sequence of *stg* mRNA Expression Patterns during Cycles 14 and Early 15, Spanning about 2 hr of Development (25°)

The right column shows *stg* mRNA patterns, visualized by in situ hybridization of a *stg* cDNA probe to whole embryos. The left column shows the same embryos stained for DNA with Hoechst 33258. Embryos A-D were hybridized with ^{35}S probe, which detects expression through several layers of tissue. Embryos E-H were hybridized with ^{3}H probe, which detects only surface expression. The anterior of each embryo is to the left.

We have labeled the regions of *stg* RNA expression with the numbers of the mitotic domains (MDs) mapped by Foe (1989). *stg* expression corresponds perfectly with these domains, but begins 25–35 min before the onset of mitosis in a given domain. A: ventral view, showing the

first zygotic *stg* expression in MD10 (10), and what is probably residual maternal RNA in the pole cells (P). B: dorsal view, just at the onset of gastrulation, about 25 min before the first mitoses. *stg* expression can be seen in MDs 1–10. C: dorsal view showing the beginning of expression in five spots within MD11, about 15 min before the first mitoses. D: dorsolateral view, showing expanded expression in MD11. The first mitoses, in MDs 1–8, are in progress in this embryo. E: ventrolateral view of an embryo the same age as D. *stg* expression can be seen in MDs 1, 2, 5, 8, 9, 11, 14, and 15. Mitoses are occurring in domains 1, 2, 5, 8, and 9, but have not yet begun in MDs 11, 14, or 15. The embryo just above this (not labeled) is slightly older and shows segmentally repeated spots of expression in MDs 16 and 17. F: ventrolateral view showing *stg* expression and mitoses in MD N. Note that expression has diminished in MDs 1–15, which have already divided. Also note the lack of expression in the amnioserosa (A), a nondividing polyploid tissue. G: lateral view, showing cycle 14 expression in MDs N and M, which are dividing. Cycle 15 expression is evident in a number of spots in the head, and in a segmental pattern in the dorsolateral epidermis and mesectoderm.

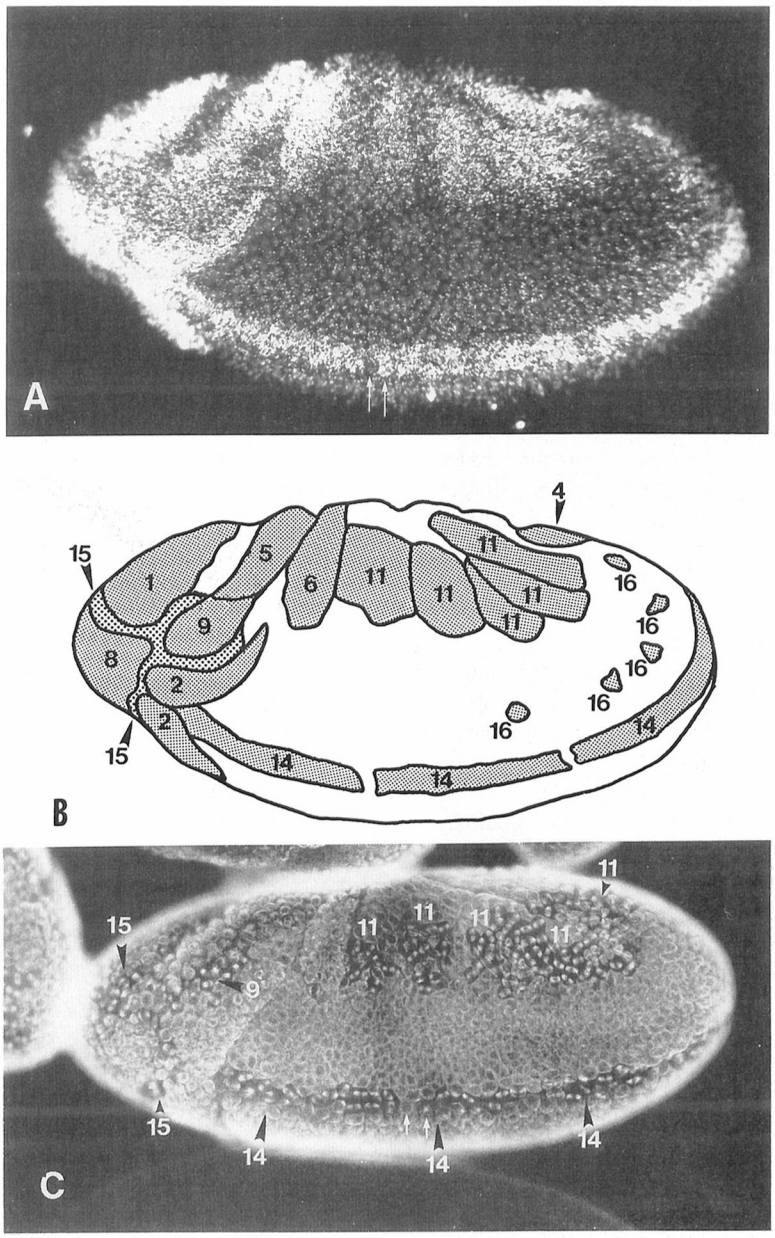

Figure 7. An Example of the Correlation of *stg* RNA Expression with the Mitotic Pattern

A: A whole, late cycle 14 embryo hybridized with ^{3}H-labeled *stg* cDNA probe. The photograph is a double exposure: silver grains show up as white dots and nuclei stained with Hoechst 33258 are gray. Arrows indicate pairs of adjacent cells containing very different levels of *stg* RNA. B: A tracing of the embryo in A, showing the correlation of *stg* expression domains (shaded) with the mitotic domains (numbers). These numbers were assigned by Foe (1989) to each mitotic domain, and indicate the relative timing of mitotic initiation in different domains. Note that *stg* RNA levels are highest in the earliest dividing domains (1–8), and lower in later dividing domains (9–16). This embryo has initiated mitosis in domains 1–6. C: A slightly older embryo stained with anti-tubulin antibodies to show mitotic spindles. In this embryo divisions have already occured in mitotic domains 1–8, and are in progress in domains 9, 11, 14, and 15 (numbers). Mitotic domains 10, 12, and 13 are not visible from this view. Small arrows indicate

adjacent cells with different mitotic states. All embryos are mounted with anterior to the left and dorsal uppermost.